Available online at www.sciencedirect.com
SCIENCE DIRECT
International Journal of Heat and Fluid Flow 27 (2006) 466–475
International Journal of HEAT AND FLUID FLOW
www.elsevier.com/locate/ijhff

Natural convection in differentially heated and partially divided square cavities with internal heat generation

H. Oztop [1], E. Bilgen *

Ecole Polytechnique, CP 6079, Centre ville, Montreal, QC, Canada H3C 3A7

Received 27 February 2005; received in revised form 21 October 2005
Available online 4 January 2006

Abstract

Heat transfer in a differentially heated, partitioned, square cavity containing heat generating fluid has been studied numerically. The vertical walls were isothermal, horizontal walls adiabatic and an isothermal partition at the reference temperature was attached to the bottom wall. Results have been obtained for various geometrical parameters specifying the height, thickness and position of the partition and for Rayleigh numbers characterizing internal and external heating from 10^3 to 10^6. Depending on the ratio of the internal and external Rayleigh numbers, two distinct regimes have been observed and studied with various geometrical parameters. Flow and temperature fields for these cases have been produced; average and local Nusselt numbers at hot and cold walls have been calculated. It is found that the flow field was modified considerably with partial dividers and heat transfer was generally reduced particularly when the ratio of internal and external Rayleigh numbers was from 10^1 to 10^2.

Keywords: Natural convection; Internal heat generation; Partitioned cavity

1. Introduction

Considerable attention is given to the study of natural convection in enclosures which are filled with volumetric heat generating fluids. The application areas are in nuclear reactor design, post-accident heat removal in nuclear reactors, geophysics and underground storage of nuclear waste and energy storage systems, among others (e.g., Baker et al., 1976; McKenzie et al., 1974).

Literature review shows various studies have been published on the mechanism of natural convection in heated enclosure containing heat generating fluids with different geometrical parameters and boundary conditions: an experimental study with equal boundary temperatures (Kulacki and Goldstein, 1972), similar to the previous study but inclined enclosures (Lee and Goldstein, 1988), a numerical study similar to that in Lee and Goldstein (1988) but with different aspect ratios (Acharya and Goldstein, 1985), a numerical study of a fluid layer with insulated side and bottom walls and rigid or free top surface (Emara and Kulacki, 1979), a numerical study with insulated side walls, heated bottom, cooled top walls (Rahman and Sharif, 2003), numerical studies with differentially heated with insulated bottom and top walls (Fusegi et al., 1992a) and with different aspect ratios (Fusegi et al., 1992b).

We will briefly review the numerical studies mentioned above. Acharya and Goldstein (1985) studied for Ra_I from 10^4 to 10^7 and Ra_E from 10^3 to 10^6, and cavity inclination angle from 30° to 90°, the latter corresponding to adiabatic bottom and top in vertical position. They found that the flow pattern changed with Ra_E/Ra_I: when this ratio was large, the flow was downward at hot and cold wall, and when small, the flow was upward at the hot wall and

* Corresponding author. Tel.: +1 514 340 4711x4579; fax: +1 514 340 5917.
E-mail address: bilgen@polymtl.ca (E. Bilgen).
[1] Present address: Department of Mechanical Engineering, Firat University, Elazig, Turkey.

0142-727X/$ - see front matter © 2005 Elsevier Inc. All rights reserved.
doi:10.1016/j.ijheatfluidflow.2005.11.003

Nomenclature

A	aspect ratio L/H	T	dimensionless temperature
c	partition position, m	T_c	cold temperature, reference temperature, °C
g	acceleration due to gravity, m/s^2	T_h	hot temperature, °C
h	partition height, m	u', v'	velocity, m/s
H	height of enclosure, m	w	partition thickness
k	heat conduction coefficient, W/mK	x, y	dimensionless coordinates
L	length of enclosure, m		
Nu	Nusselt number	*Greek symbols*	
Q	rate of internal heat generation per unit volume	α	thermal diffusivity, m^2/s
p	pressure, N/m^2	β	coefficient of thermal expansion of fluid, 1/K
Pr	Prandtl number	ν	kinematic viscosity, m^2/s
Ra_I	internal Rayleigh number	ϕ	general variable
Ra_E	external Rayleigh number		

downward at the cold wall. Rahman and Sharif (2003) studied numerically the case in inclined rectangular cavities with heated bottom and cooled top walls and insulated sides. Ra_I and Ra_E were 2×10^5 and the aspect ratio from 0.25 to 4. They found that for $Ra_E/Ra_I > 1$, the convective flow and heat transfer was almost the same as that in a cavity without internal heat generating fluid and they observed similar results as in Acharya and Goldstein (1985).

Following the experimental studies by Kawara et al. (1990) with a differentially heated square cavity containing a heat generating fluid of $Pr = 5.85$, Fusegi et al. (1992a,b) numerically studied the same problem at high external and internal Rayleigh numbers, Ra_E set at 5×10^7 and Ra_I varied from 10^9 to 10^{10}. They found a broad agreement with the experimental results and identified similar patterns as reported in Acharya and Goldstein (1985).

There is a renewed interest in energy conservation and energy storage systems using fundamental principles of heat transfer in enclosures with volumetric heat generating fluids. The presence of a partial divider in a differentially heated enclosures containing heat generating fluid adds an additional dynamic to overall convection characteristics, which we will study in the present work. Both Ra_I and Ra_E will be varied from 10^3 to 10^6 and various partial divider geometry and position will be used. We will carry out a numerical study and analyze the results to examine the flow patterns and heat transfer. Thus, we will provide additional basic design information.

2. Problem definition

Schematic of the problem with coordinate system and boundary conditions is shown in Fig. 1. It is a square enclosure with isothermal vertical walls at T_h and T_c, and adiabatic horizontal walls. It is filled with a uniform heat generating fluid with volumetric rate of Q. An isothermal solid partition of h by w at T_c is placed at a distance c from the origin as shown in the figure.

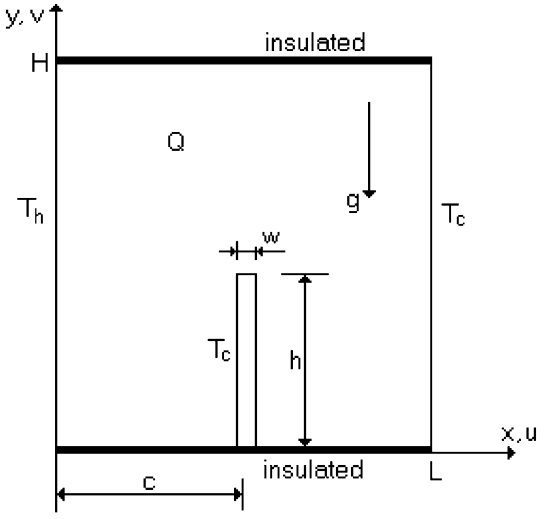

Fig. 1. Problem definition, the coordinate system and boundary conditions.

3. Governing equations

We assume that the fluid is Newtonian and incompressible, the flow is laminar, and the effect of viscous dissipation is negligible. Further, the gravity acts in the vertical direction, fluid properties are constant and fluid density variations are neglected except in the buoyancy term, and radiation heat transfer is negligible. With these assumptions the non-dimensional governing equations are

$$\frac{\partial u}{\partial x}+\frac{\partial v}{\partial y}=0 \tag{1}$$

$$u\frac{\partial u}{\partial x}+v\frac{\partial u}{\partial y}=-\frac{\partial P}{\partial x}+Pr\left(\frac{\partial^2 u}{\partial x^2}+\frac{\partial^2 u}{\partial y^2}\right) \tag{2}$$

$$u\frac{\partial v}{\partial x}+v\frac{\partial v}{\partial y}=-\frac{\partial P}{\partial y}+Pr\left(\frac{\partial^2 v}{\partial x^2}+\frac{\partial^2 v}{\partial y^2}\right)+\frac{Ra_E}{Pr}T \tag{3}$$

$$u\frac{\partial T}{\partial x}+v\frac{\partial T}{\partial y}=\left(\frac{\partial^2 T}{\partial x^2}+\frac{\partial^2 T}{\partial y^2}\right)+\frac{Ra_I}{Ra_E Pr} \tag{4}$$

In derivation of the non-dimensional equations the following dimensionless variables are defined and used, where the primed parameters are dimensional

$$(x,y)=(x',y')/H,\quad u,v=(u',v')H/\alpha$$
$$T=(T'-T_c)/\Delta T,\quad \text{with } \Delta T=T_h-T_c\quad t=t'\alpha/H^2 \tag{5}$$

3.1. Boundary conditions

On the solid walls no-slip boundary conditions are applied. The relevant boundary conditions are

On the left wall $x=0,\ 0<y<1,\ u=0,\ v=0,\ T=1$ (6a)

On the right wall $x=1,\ 0<y<1,\ u=0,\ v=0,\ T=0$ (6b)

On the bottom wall $y=0,\ 0<x<1,\ u=0,\ v=0,\ \partial T/\partial y=0$ (6c)

On the top wall $y=1,\ 0<x<1,\ u=0,\ v=0,\ \partial T/\partial y=0$ (6d)

On the partition surface $u=0,\ v=0,\ T=0$ (6e)

Dimensionless numbers for the system can be written as follows:

$$Pr=\frac{v}{\alpha},\quad Ra_E=\frac{g\beta\Delta TH^3}{\alpha v},\quad Ra_I=\frac{g\beta QH^5}{\alpha vk} \tag{7}$$

The local Nusselt number is

$$Nu_y=-(\partial T/\partial x)_w \tag{8}$$

The average Nusselt number is calculated by integrating the local Nusselt number along the wall

$$Nu=\int_0^1 Nu_y\,dx \tag{9}$$

4. Numerical methods

A modified version of the general purpose SAINTS software (Software for Arbitrary Integration of Navier–Stokes Equation with a Turbulence and Porous Media Simulator Nakayama (1995)) was used to solve Eqs. (1)–(4) with the boundary conditions Eqs. (6). SAINTS makes use of the SIMPLE algorithm of Patankar (1980). In the solution, the linear algebraic equation solution procedure is adopted in which TDMA, line-by-line relaxation method is used to solve algebraic equations. Under-relaxation factors of 0.3, 0.3, 0.2 and 0.5 were used for u-velocity, v-velocity, pressure and temperature respectively. Grid convergence was studied with grid sizes from 24×24 to 72×72. Grid independence was achieved within 1.2% with a grid size of 48×48 with which the majority of runs was carried out. The convergence criterion employed was max $(|\phi^{i+1}-\phi^i/\phi^i|)<10^{-7}$ where i and $i+1$ are two consecutive iterations and where ϕ stands for u, v and T.

Table 1
Comparison of the results with the benchmark solution (De Vahl Davis and Jones, 1983)

Ra	De Vahl Davis and Jones (1983)		Present study	
	Nu_m	ψ	Nu_m	ψ
10^4	2.24	5.098	2.22	5.072
10^5	4.523	9.64	4.46	9.62
10^6	8.928	16.691	8.66	16.961

Table 2
Comparison of Nusselt number and stream functions with (Shim and Hyun, 1997)

Ra_I	Ra_E	Shim and Hyun (1997)			Present results		
		Ψ_{max}	Ψ_{min}	Nu_m	Ψ_{max}	Ψ_{min}	Nu
10^6	10^5	1.56	−17	−0.01	1.61	−16.7	0.1
10^7	10^5	16.4	−24.5	−66	15.4	−23.2	−59

4.1. Validation

Some calculations were made to compare results from the code with data in the literature, one with the benchmark solution of natural convection in fluid media in a square enclosure De Vahl Davis and Jones (1983) and the other with the case of differentially heated cavity with internal heat generation Shim and Hyun (1997). In the first case, with $Ra_I=0$, the results obtained with the code show good agreement as presented in Table 1. The deviations in Nusselt number are from 0.89% for $Ra=10^4$ to 3.00% for $Ra=10^6$, and in the stream function it is from 0.51 to −1.61% respectively. In the second case, the results from the code also show acceptable agreement as can be seen in Table 2. The deviations are 10.6% in Nusselt number and 6.10% and 5.31% in the maximum and minimum stream function respectively.

5. Results and discussion

For differentially heated square cavity with internal heat generating fluid at $Pr=0.71$ and a cold partition, the governing parameters are Ra_I, Ra_E, and partition geometrical parameters are h/H, w/H and c/H. Ra_I and Ra_E are both varied from 10^3 to 10^6, the height of the partition, h/H varied from 0 (no partition) to 0.75, its thickness, w/H from 0.01 to 0.75 and its position, c/H from 0.25 to 0.75.

5.1. Flow and temperature fields

Flow and temperature fields for the case without partition and various Ra_I, Ra_E were obtained as reference (not shown in figures). The cases with $Ra_I=10^5$, $Ra_E=10^4$ and $Ra_I=10^5$, $Ra_E=10^3$ were exactly mirror images of Figs. 6 and 5 of Acharya and Goldstein (1985) in which their left side is cold wall and the right is hot. We observed that for a constant $Ra_I=10^5$, the effect of

external heating by decreasing Ra_E from 10^4 to 10^3 was to cause a transition from the pattern with a dominating cell to a quasi-symmetric one with two counter rotating cells. By increasing both Ra_I and Ra_E by an order of 10, the flow pattern was almost the same except with stronger circulation. In contrast, the flow and temperature fields of the same as in the reference case but with $w = 0.01$, $h = 0.5$ and $c = 0.5$ are modified considerably. The flow field for $Ra_I = 10^5$ and $Ra_E = 10^4$ presented on the left side of Fig. 2(a) shows a clockwise circulation in the left hand side of the cavity, upward on the hot wall, which continues following the adiabatic top wall and downward on the cold wall filling the right half of the cavity. The fluid rises along a secondary cell at the partition and with a sharp turn at the upper end of it, and completes the circulation. Weak counterclockwise circulations are formed at the left upper corner and on the right of the partition. $|\Psi_{ext}| = 2.52$ at $x = 0.74$, $y = 0.69$. The isotherms on the right show, as

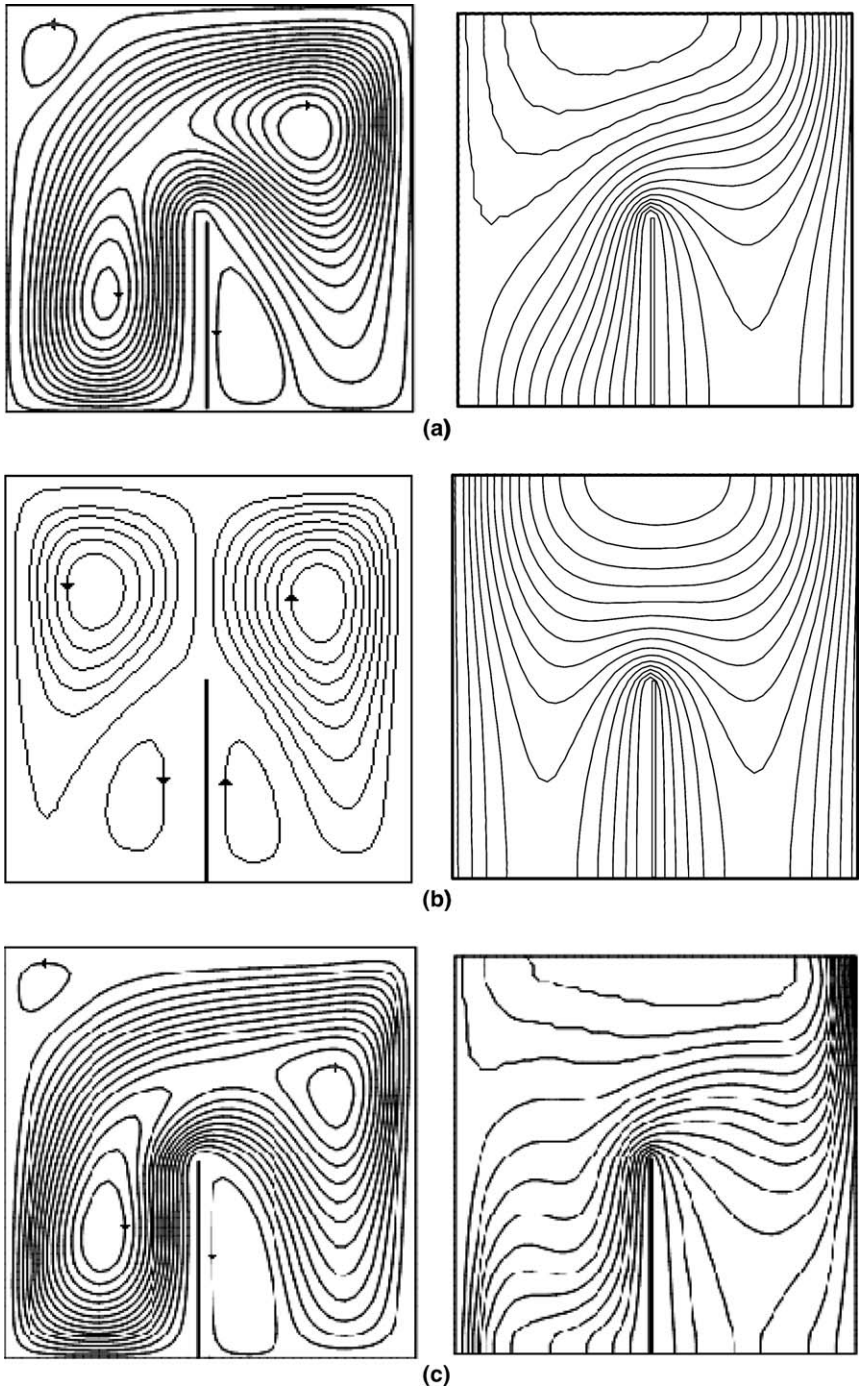

Fig. 2. Streamlines (on the left) and isotherms (on the right) showing the effect of Rayleigh numbers. $h/H = 0.50$, $w/H = 0.01$, $c/H = 0.50$: (a) $Ra_I = 10^5$, $Ra_E = 10^4$, (b) $Ra_I = 10^5$, $Ra_E = 10^3$, (c) $Ra_I = 10^6$, $Ra_E = 10^5$.

expected, that the temperature gradient is increasing along the cold wall as well as on the left hand side of the partition, both due to cooling of the fluid. For this case $Ra_I/Ra_E = 10$. For $Ra_I/Ra_E = 100$ with $Ra_I = 10^5$ and $Ra_E = 10^3$ the flow and temperature fields in Fig. 2(b) show quite symmetric patterns. Since Ra_E is small in this case a quasi-conduction dominated regime is observed. We see two major circulations, a counter clockwise circulation on the hot wall and a clockwise circulation on the cold wall. Two weak circulations are formed around the partition. In this case, $|\Psi_{ext}| = 1.54$ at $x = 0.77$, $y = 0.70$. The isotherms on the right show quasi-conductive regime with almost parallel isotherms across the cavity. Like in Fig. 2(a), for $Ra_I/Ra_E = 10$ but with $Ra_I = 10^6$ and $Ra_E = 10^5$, the flow and temperature fields are presented in Fig. 2(c). Due to high Ra_E in this case, the flow field is with more rigorous circulation, $|\Psi_{ext}| = 10$ at $x = 0.23$, $y = 0.29$, although the pattern of the streamlines is similar to that of Fig. 2(a). In this case, the weak circulation at the left upper corner became still weaker and the other one

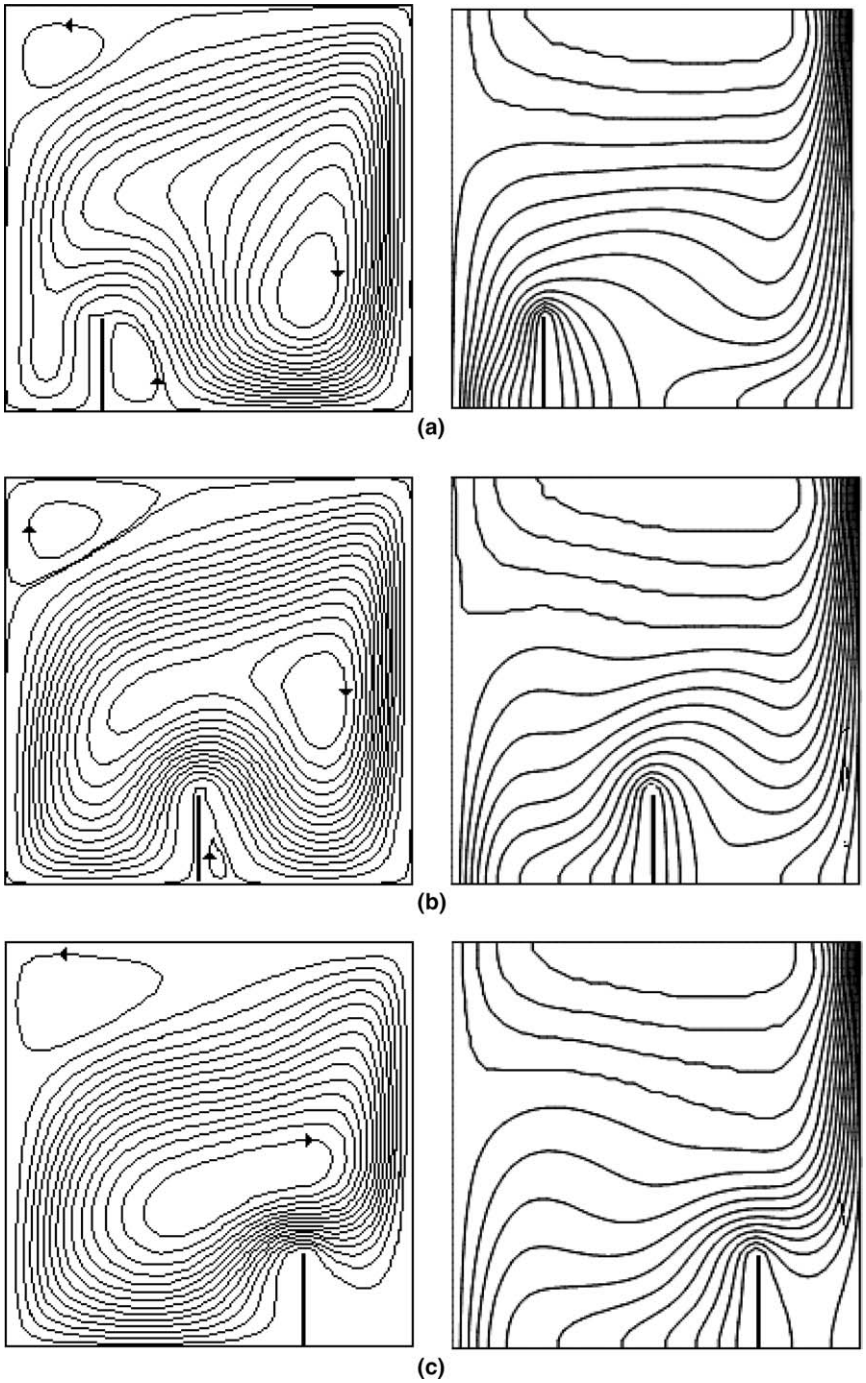

Fig. 3. Streamlines (on the left) and isotherms (on the right) showing the effect of the partition position on heat transfer and fluid flow. $h/H = 0.2$, $w/H = 0.01$ and $Ra_I = 10^6$, $Ra_E = 10^5$: (a) $c/H = 0.25$, (b) $c/H = 0.50$, (c) $c/H = 0.75$.

behind the partition became stronger. The isotherms on the right show a stratified fluid flow and the temperature gradients on the hot and cold walls are large.

Effect of the partition height and position is studied using a partition with $w/H = 0.01$, $h/H = 0.2$, and its position at $c/H = 0.25$, 0.50 and 0.75. The flow and temperature fields for $Ra_I = 10^6$ and $Ra_E = 10^5$ are presented in Fig. 3(a)–(c). The flow field of the case with the partition at the center, $c/H = 0.50$, shown in Fig. 3(b) has a clockwise rotating single cell, which is a dominant circulation in the cavity, $|\Psi_{ext}| = 12$ at $x = 0.77$, $y = 0.46$. Two weak counterclockwise rotating cells are formed as we have seen before in Fig. 2(c) at the left upper corner and behind the partition, though the former is stronger and the latter is very weak due to small partition height. The isotherms on the right have a similar pattern as those of Fig. 2(c) except, because of the shorter partition the stratification fills the three quarter of the cavity. The cases at $c/H = 0.25$ and 0.75 are presented in Fig. 3(a) and (c) respectively. For the case with $c/H = 0.25$, the flow field is modified by the partition located near the hot wall, but the flow pattern is very similar to that of Fig. 3(b), although the strength of circulation is quite different with $|\Psi_{ext}| = 12.5$ at $x = 0.74$, $y = 0.29$. The isotherms on the right show a stratified flow, with high temperature gradients at the cold wall as well as on the partition very similar to that of Fig. 2(b). For the case with $c/H = 0.75$ in Fig. 3(c), the flow pattern changed markedly since the partition blocks the flow coming from the cold wall in the lower part of the cavity. $|\Psi_{ext}| = 13.8$ at $x = 0.52$, $y = 0.39$ for this case. The isotherms show a stratified flow and their pattern is similar to those in Fig. 3(b).

Effect of the partition thickness, w/H on the flow and temperature fields was studied for $Ra_I = 10^6$ and $Ra_E = 10^5$, $h/H = 0.5$, $c/H = 0.5$ and variable $w/H = 0.25$, 0.50 and 0.75 respectively (not shown in figures). For $w/H = 0.25$ we observed that the streamlines showed a dominant clockwise circulation in the cavity with $|\Psi_{ext}| = 7.35$ at $x = 0.25$, $y = 0.64$, which indicated that the strength of the circulation had shifted to the right due to vigorous cooling at the cold wall. The heating at the left wall and the cooling on the partition was also more vigorous compared to those with a thin partition of Fig. 2. The isotherms were indicative of high temperature gradients at the upper part of the cold wall and at the lower part of the hot wall as well as on the cold partition surfaces where the fluid is cooled. For $w/H = 0.50$, the partition blocked practically lower half of the cavity on the right hand side where a conduction regime dominated. The fluid cooled on the upper part of the cold wall circulated downwards along it,

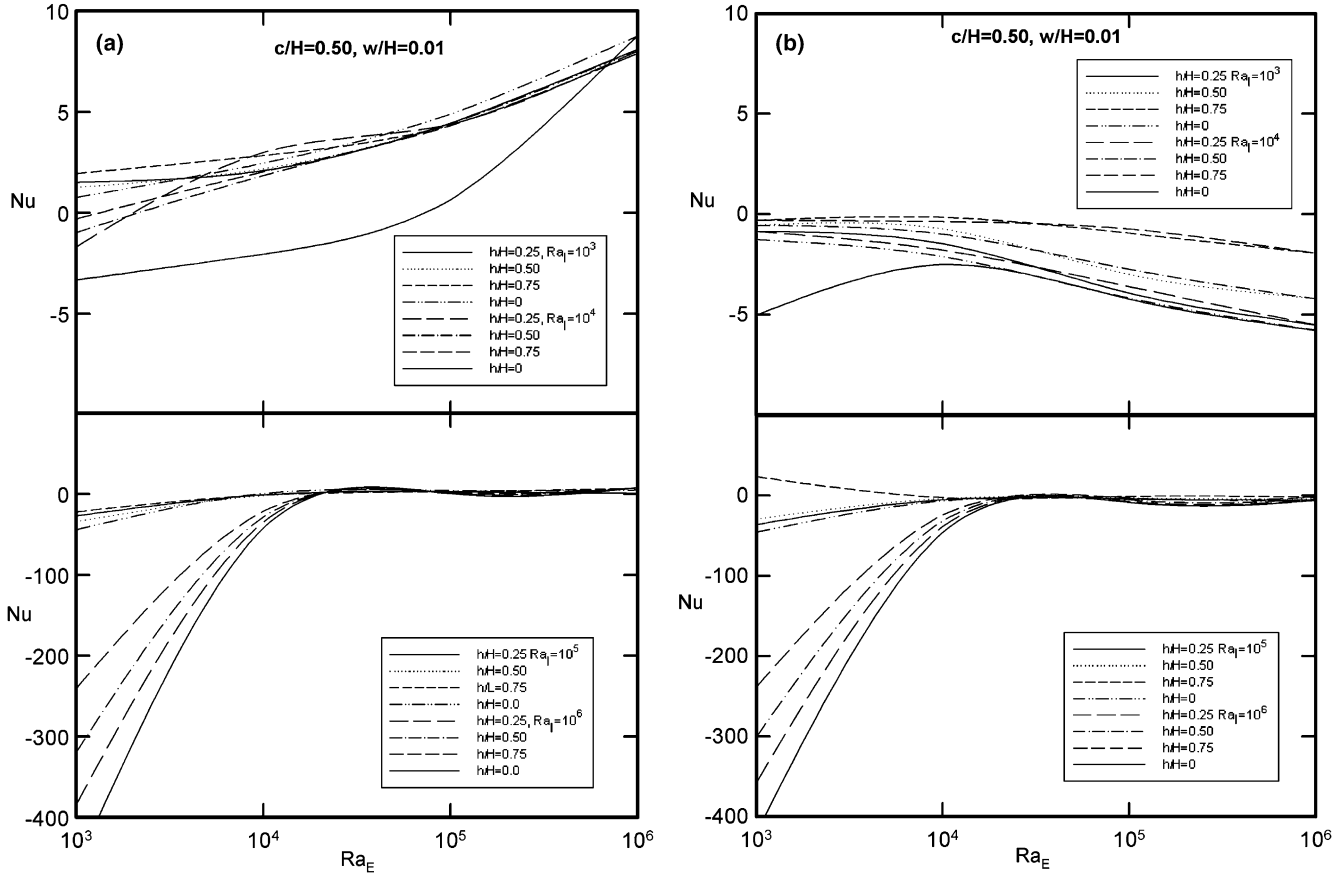

Fig. 4. Nusselt number as a function of the external Rayleigh number for the case of $c/H = 0.50$, $w/H = 0.01$ and c/H variable. The upper figure is for $Ra_I = 10^3$ and 10^4 and the lower for $Ra_I = 10^5$ and 10^6: (a) on the hot wall at $x = 0$, (b) on the cold wall at $x = 1$.

forming a single counterclockwise cell with two cells inside it with $|\Psi_{ext}| = 6.38$ at $x = 0.79$, $y = 0.73$. The isotherms showed that the cooling was along the cold wall and the partition surfaces were swept by the fluid. For $w/H = 0.75$, the partition almost filled the lower part of the cavity with fluid flow confined to the upper part of the cavity where a single clockwise rotating cell was observed with $|\Psi_{ext}| = 5.99$ at $x = 0.78$, $y = 0.74$. In the lower parts between the partition and the walls, there seemed to be no fluid flow. The isotherms were those of a stratified cavity, with conduction regime between the partition and the hot wall.

5.2. Heat transfer

Average Nusselt number on the hot and cold walls calculated by Eq. (9) is presented in Figs. 4–6 as a function of the external Rayleigh number, Ra_E from 10^3 to 10^6 for various geometrical parameters, h/H, w/H, c/H and the internal Rayleigh number, Ra_I from 10^3 to 10^6. Figs. 4(a)–6(a) are for Nusselt number at the left wall, i.e. hot wall at $x = 0$ and Figs. 4(b)–6(b) are for Nusselt number at the right wall, i.e. cold wall at $x = 1$. We note that following the definitions of Rayleigh numbers in Eq. (7), $Ra_E \sim \Delta T$ and $Ra_I \sim Q$. For $Nu > 0$, the heat transfer on the hot or cold wall is into the cavity and for $Nu < 0$ it is out of the cavity. As we have seen in Figs. 2 and 3, the ratio Ra_I/Ra_E is a parameter affecting the flow and temperature fields in the cavity and is also indicative of the heat transfer direction. As we have observed earlier, there are two distinct regimes: For $Ra_I/Ra_E \ll 1$, the external heating is important and the heat transfer is an increasing function of Ra_E, and for $Ra_I/Ra_E \gg 1$, the heat generation in the cavity becomes dominant with respect to the external heating and the heat transfer becomes an increasing function of increasing Ra_I. For clarity of presentation and to reveal better these two regimes, the results of Nusselt number versus external Rayleigh number will be plotted in separate figures for $Ra_I = 10^3$ and 10^4, and for $Ra_I = 10^5$ and 10^6.

We note that for $h/H = 0$, we have natural convection in a differentially heated square cavity containing a fluid with uniform heat generation without a partition, which has been studied in the literature (Acharya and Goldstein, 1985; Fusegi et al., 1992b). It has been shown that depending on Ra_I/Ra_E ratio, complex flow patterns have been observed and the heat dissipation is mainly through the cold wall but may be also through the hot wall. Following our observations in Figs. 2 and 3, it is expected that the dissipation in the same cavity with an isothermal partition attached on the bottom wall will be through the cold wall

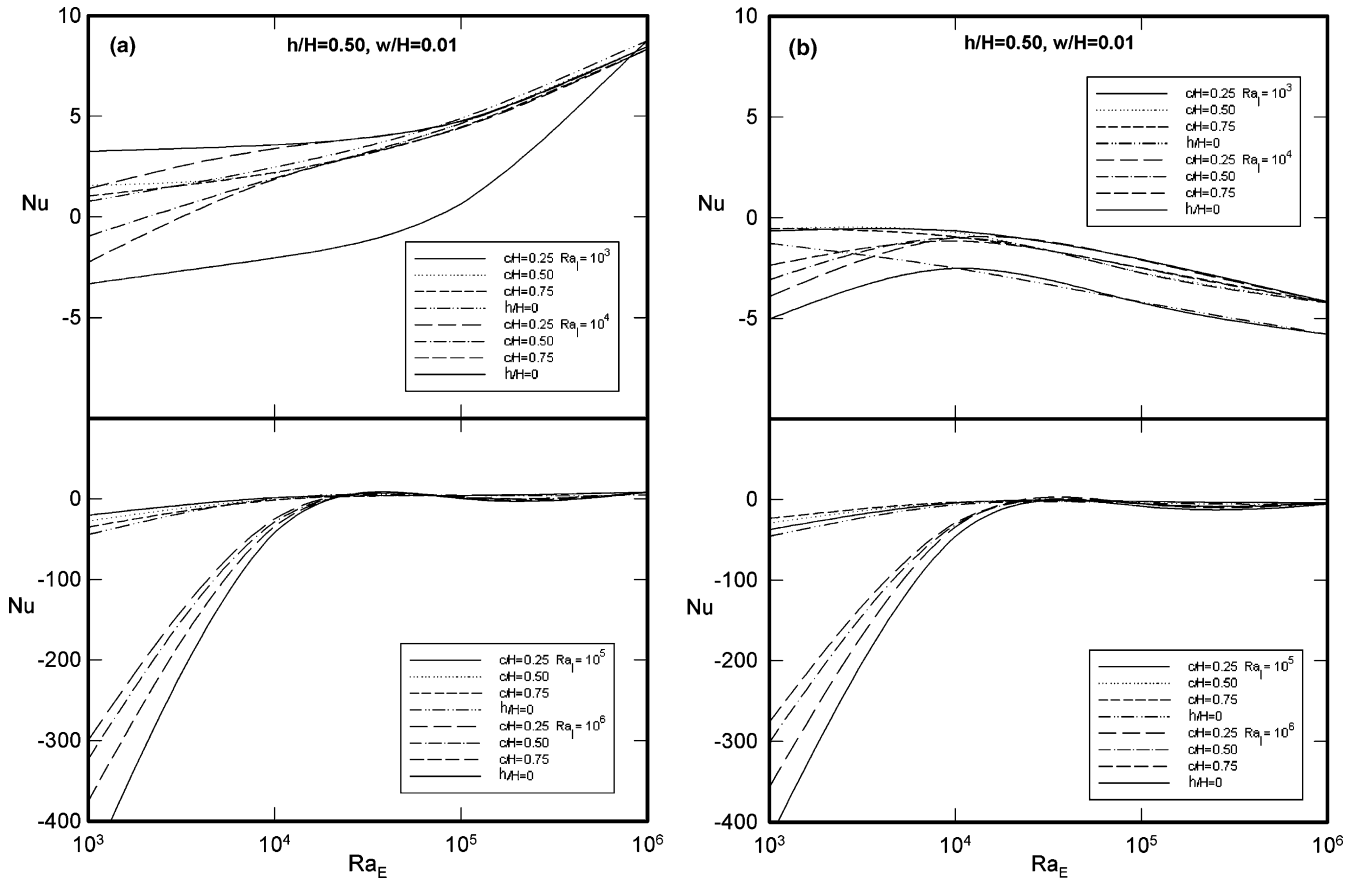

Fig. 5. Nusselt number as a function of the external Rayleigh number for the case of $h/H = 0.50$, $w/H = 0.01$ and c/H variable. The upper figure is for $Ra_I = 10^3$ and 10^4 and the lower for $Ra_I = 10^5$ and 10^6: (a) on the hot wall at $x = 0$, (b) on the cold wall at $x = 1$.

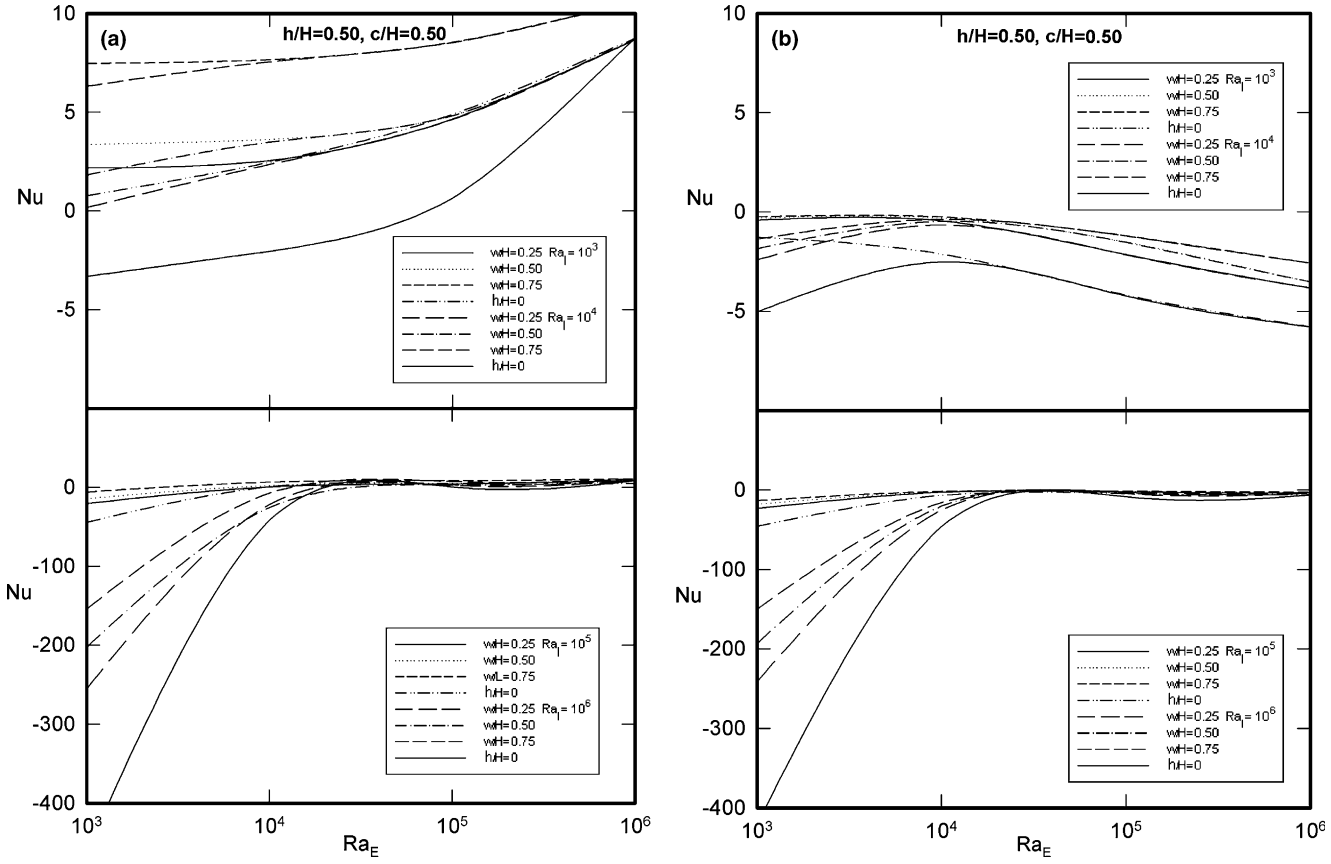

Fig. 6. Nusselt number as a function of the external Rayleigh number for the case of $h/H = 0.50$, $c/H = 0.50$ and w/H variable. The upper figure is for $Ra_I = 10^3$ and 10^4 and the lower for $Ra_I = 10^5$ and 10^6: (a) on the hot wall at $x = 0$, (b) on the cold wall at $x = 1$.

as well as cold partition wall and in some cases through the hot wall. To see the effect of various governing parameters on heat transfer, various cases will be presented and discussed next.

To see the effect of the partition length, h/H on heat transfer as a function of Ra_E, the case with $c/H = 0.50$ and $w/H = 0.01$ constant and h/H variable is presented in Fig. 4(a). The upper figure is for $Ra_I = 10^3$ and 10^4 and the lower one is for $Ra_I = 10^5$ and 10^6, in both h/H is varied from zero (no partition) to 0.75. In the upper figure, Ra_E up to about 10^5, the effect of partition height is easily discernible and generally the heat transfer is into the cavity at $x = 0$, an expected trend since the external heating dominates at low Ra_I. For $Ra_I = 10^3$, the heat transfer is almost the same for $h/H = 0.25$ and 0.50 but it is higher for 0.75. For $Ra_I = 10^4$, a similar trend is observed though at $Ra_E = 10^3$ the heat transfer became negative, i.e. out of the cavity, and the heat transfer is an increasing function of h/H. In the lower figure for $Ra_I = 10^5$ and 10^6, we see that Ra_E up to about 3×10^5, a similar trend in both $Ra_I = 10^5$ and 10^6 is observed with heat transfer out of the cavity. Indeed at low Ra_E, the ratio Ra_I/Ra_E has an order of 10^2–10^3, and the internal heat generation is dominant in the cavity. As expected, the heat transfer is generally reduced by the presence of partition. For $Ra_I = 10^6$ for example, it is clearly seen that the heat transfer through the hot wall is highest without partition and gradually reduced with increasing partition height. This is expected because increasing height of the partition divides the cavity into two sections preventing heat transfer from the whole cavity. We note that although it is not discernible in this and following figures, the same trend exist at high Ra_E.

Heat transfer results on the cold wall at $x = 1$ are presented in Fig. 4(b) where we can observe in all cases that for low Ra_I in the upper figure, without and with partition, the heat transfer is out of the cavity. The heat transfer increases with increasing Ra_E because of increasing external heating while the internal heating strength is kept constant. For $Ra_I = 10^5$ and 10^6 in the lower figure, heat transfer is also out of the cavity in all cases except for $Ra_I = 105$, $h/H = 0.75$ at low Ra_E. It is more discernible for Ra_E smaller than about 3×10^5 where the heat transfer is reduced by the presence of partition. As we observed in Fig. 4(a), the heat transfer with partition is reduced proportionately with h/H.

The effect of the partition position on the heat transfer on the hot and cold walls for $h/H = 0.5$, $w/H = 0.01$ constant and c/H variable is presented in Fig. 5(a) on the hot wall and in Fig. 5(b) on the cold wall for Ra_I and Ra_E from 10^3 to 10^6. Following the results with $c/H = 0.5$ in Fig. 4, the trend is similar in both figures, i.e., in general, the heat transfer is into the cavity for low Ra_I

of 10^3 and 10^4, and out of the cavity for high Ra_I of 10^5 and 10^6 when Ra_E is smaller than about 3×10^5 in the latter case. The heat transfer is generally modified by the position of partition. For $Ra_I = 10^6$ for example, it is clearly seen that the heat transfer through the hot wall is highest without partition and gradually reduced when the partition position becomes closer to the hot wall. Following our observation in Fig. 3 this trend is expected because the flow is restricted more and more when the partition is placed closer to the hot wall.

Heat transfer at the cold wall at $x = 1$ is presented for this case in Fig. 5(b) where we see that similar to the case in Fig. 4(b), it is out of the cavity for all cases, an expected result since external heating enhances the heat transfer due to internal heat generation at the cold wall. For example, for $Ra_I = 10^4$ in the upper figure, the heat transfer is reduced by the partition with respect to the case without partition at low Ra_E numbers up to about 10^4. The reduction is enhanced as the partition becomes closer to the cold wall, as expected from the observations made earlier in Fig. 3. The same is true also for $Ra_I = 10^5$ and 10^6 in the lower figure, in which case the effect is discernible up to about $Ra_E = 3\times10^4$.

The effect of the partition thickness on the heat transfer with $h/H = 0.5$, $c/H = 0.5$ constant and w/H variable is presented in Fig. 6(a) on the hot wall at $x = 0$ and in Fig. 6(b) on the cold wall at $x = 1$ for Ra_I and Ra_E from 10^3 to 10^6 Again the case without partition ($h/H = 0$) is plotted for reference. For low Ra_I of 10^3 and 10^4 in the upper figure, as the partition thickness increased, the internal heat generation's effect becomes reduced and the heat transfer is into the cavity due to the increased external heating. For high Ra_I of 10^5 and 10^6, when Ra_E is smaller than about 3×10^5, in the lower figure, the heat transfer is from the cavity through the hot wall and the trend is reversed. The heat transfer is highest for the case without partition and gradually decreased with increasing partition thickness, which can be seen clearly for $Ra_I = 10^6$ at low Ra_E. The reason is that as the partition thickness increased, it fills the lower part of the cavity as a result of which the internal heat generation becomes reduced.

The effect of the thickness on the heat transfer through the cold wall at $x = 1$ is shown in Fig. 6(b). The heat transfer through the cold wall is out of the cavity for all cases and the reduction of heat transfer with respect to the case without partition is an increasing function of the partition thickness.

5.3. Local Nusselt number at hot and cold walls

Local Nusselt number at $x = 0$ and $x = 1$ is calculated using Eq. (8). For the same case of Fig. 2 with $h/H = 0.50$, $c/H = 0.50$ and $w/H = 0.01$ it is presented in the upper figure of Fig. 7 and for the same case of Fig. 3 with $Ra_I = 10^6$, $Ra_E = 10^5$, $h/H = 0.20$, $w/H = 0.01$ constant in the lower figure of Fig. 7. We notice that for the case of Fig. 2(a), the heat transfer at $x = 0$ is into the cavity

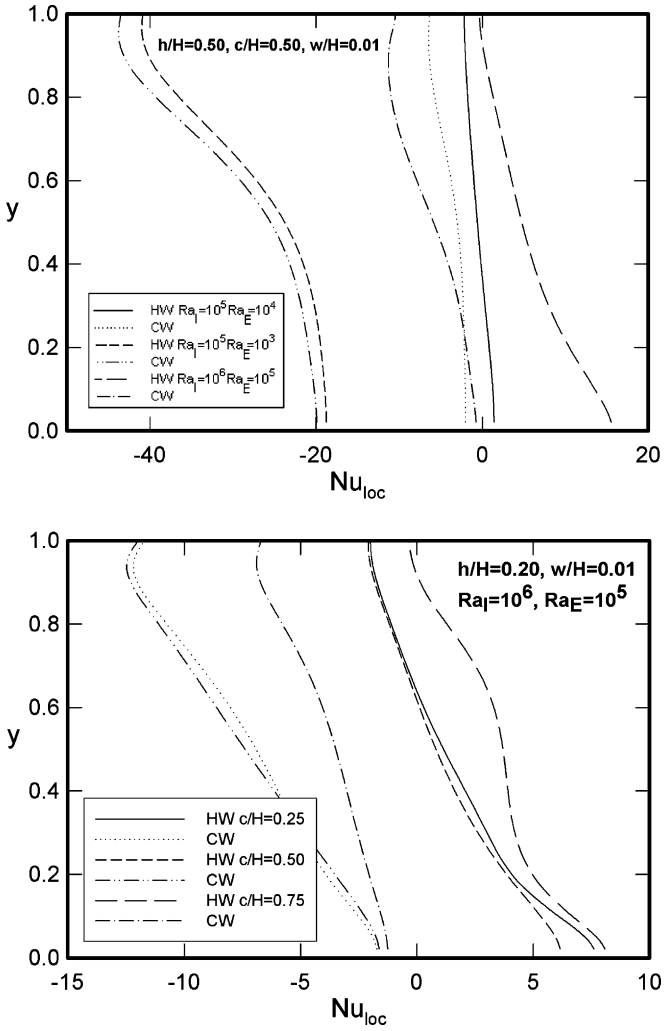

Fig. 7. Local Nusselt number along the hot at $x = 0$ and cold wall at $x = 1$, designated as HW = hot wall and CW = cold wall in the figures respectively. The upper figure is for $h/H = 0.50$, $c/H = 0.50$ and various Ra_I and Ra_E. The lower figure is for $h/H = 0.20$, $w/H = 0.01$, and $Ra_I = 10^6$, $Ra_E = 10^5$ with $c/H = 0.25$, 0.50 and 0.75.

at the lower part and becomes out of the cavity at the upper part. The fluid coming from the cold wall at $x = 1$ and the partition at relatively low temperature is heated further by the external heating up to $y = 0.4$ after which the heat transferred from the hot fluid to the wall. It is seen in Fig. 2(a) that the mechanism of heat transfer at the upper part is by counter circulating corner cell of hot fluid. The heat transfer at $x = 1$ is out of the cavity and stronger at the upper part, which is also seen by isotherms in Fig. 2(a). In the case of Fig. 2(b), the heat transfer at $x = 0$ and $x = 1$ is almost similar and out of the cavity, relatively low at the lower part, almost twice as much at the upper part. The case of Fig. 2(c), which is an enhanced case of that of Fig. 2(a), has a very similar mechanism and appearance to the first case discussed above.

For the case of Fig. 3, local Nusselt number at $x = 0$ and $x = 1$ is presented in the lower figure, which shows that for the partition position of $c/H = 0.25$, the heat transfer at the

lower part at $x = 0$ is from the hot wall to the relatively cold fluid up to $y = 0.65$ thereafter the heat transfer is from the hot fluid to the wall by counterclockwise rotating corner cell. The heat transfer at $x = 1$ for this case is from the hot fluid to the cold wall, there is a stratification and the heat transfer is stronger at the upper part as it can be seen from the high temperature gradients in Fig. 3(a). Local Nusselt number variation for $c/H = 0.50$ corresponding to Fig. 3(b), seems to be very similar to the previous case. For the partition position at $c/H = 0.75$, closer to the cold wall, the cooled fluid coming from the cold surface at $x = 1$ sweeps the cold partition surface, then it is heated along the hot wall at $x = 0$ all the way up, it circulates then along the adiabatic top wall, it is cooled down at the cold wall especially at the upper part of it, completing the circulation.

6. Conclusions

Heat transfer by natural convection in differentially heated square cavity with uniform internal heat generation and with an isothermal partition attached on the bottom wall has been studied numerically. The conservation of mass, momentum and energy equations have been solved using the control volume method and the Simple algorithm. The geometrical parameters of the cold partition, namely its height, thickness and position have been varied from zero to 0.75, and results have been obtained for the internal and external Rayleigh numbers from 10^3 to 10^6. Two distinct regimes have been identified: For $Ra_I/Ra_E \ll 1$, the heat transfer has been an increasing function of the external Rayleigh number with heat transfer direction as in the case of a differentially heated cavity, from hot to cold wall. For $Ra_I/Ra_E \gg 1$, the heat transfer has been an increasing function of the internal Rayleigh number and its direction out from the cavity at both hot and cold walls. Generally in the presence of a cold partition the heat transfer is reduced and the heat reduction is gradually increased with increasing partition height and thickness. The heat transfer is reduced more effectively when the partition is closer to the hot or cold wall.

References

Acharya, S., Goldstein, R.J., 1985. Natural convection in an externally heated square box containing internal energy sources. J. Heat Transfer 107, 855–866.

Baker Jr., L., Faw, E.F., Kulacki, F.A., 1976. Postaccident heat removal—Part I: Heat transfer within an internally heated, nonboiling liquid layer. Nucl. Sci. Eng. 61, 222–230.

De Vahl Davis, G., Jones, J.P., 1983. Natural convection in a square cavity: A comparison exercise. Int. J. Numer. Meth. Fluids 3, 227–248.

Emara, A.A., Kulacki, F.A., 1979. A numerical investigation of thermal convection in a heat-generating fluid layer. ASME Paper No. 79-HT-103.

Fusegi, T., Hyun, J.M., Kuwahara, K., 1992a. Natural convection in a differentially heated square cavity with internal heat generation. Numer. Heat Transfer A 21, 215–229.

Fusegi, T., Hyun, J.M., Kuwahara, K., 1992b. Numerical study of natural convection in a differentially heated cavity with internal heat generation: effects of the aspect ratio. J. Heat Transfer 114, 773–777.

Kawara, Z., Kishiguchi, I., Aoki, N., Michiyoshi, I., 1990. Natural convection in a vertical fluid layer with internal heating. In: Proc. 27th Natl. Heat Transfer Symp. Japan. vol. II, pp. 115–117.

Kulacki, F.A., Goldstein, R.J., 1972. Thermal convection in a horizontal fluid layer with uniform volumetric energy sources. J. Fluid Mech. 55, 271–287.

Lee, J.-H., Goldstein, R.J., 1988. An experimental study on natural convection heat transfer in an inclined square enclosure containing internal energy sources. J. Heat Transfer 110, 345–349.

McKenzie, D.P., Roberts, J.M., Weiss, N.O., 1974. Convection in the Earth's mantle: towards a numerical solutions. J. Fluid Mech. 62, 465–538.

Nakayama, A., 1995. PC-Aided Numerical Heat Transfer and Convective Flow. CRC Press.

Patankar, S.V., 1980. Numerical Heat Transfer and Fluid Flow. Hemisphere/McGraw-Hill, Washington D.C.

Rahman, M., Sharif, M.A.R., 2003. Numerical study of laminar natural convection in inclined rectangular enclosures of various aspect ratios. Numer. Heat Transfer A 44, 355–373.

Shim, Y.M., Hyun, J.M., 1997. Transient confined natural convection with internal heat generation. Int. J. Heat Fluid Flow 18, 328–333.